HHS Public Access

Author manuscript

J Immunol. Author manuscript; available in PMC 2015 April 16.

Published in final edited form as:

J Immunol. 2010 October 15; 185(8): 4896–4903. doi:10.4049/jimmunol.1001857.

NF-κB Activation Limits Airway Branching through Inhibition of Sp1-Mediated Fibroblast Growth Factor-10 Expression

John T. Benjamin[*,†,1], **Billy J. Carver**[*,‡], **Erin J. Plosa**[*], **Yasutoshi Yamamoto**[*], **J. Davin Miller**[*,†], **Jin-Hua Liu**[*], **Riet van der Meer**[*], **Timothy S. Blackwell**[‡,§,¶,‖], and **Lawrence S. Prince**[*,†,‡]

[*]Division of Neonatology, Department of Pediatrics, Vanderbilt University School of Medicine, Nashville, TN 37232

[§]Division of Allergy, Pulmonary, and Critical Care Medicine, Department of Medicine, Vanderbilt University School of Medicine, Nashville, TN 37232

[¶]Department of Cancer Biology, Vanderbilt University School of Medicine, Nashville, TN 37232

[‡]Department of Cell and Developmental Biology, Vanderbilt University School of Medicine, Nashville, TN 37232

[‖]Department of Veterans Affairs Medical Center, Nashville, TN 37243

[†]Department of Pediatrics, University of Alabama at Birmingham, Birmingham, AL 35233

Abstract

Bronchopulmonary dysplasia (BPD) is a frequent complication of preterm birth. This chronic lung disease results from arrested saccular airway development and is most common in infants exposed to inflammatory stimuli. In experimental models, inflammation inhibits expression of fibroblast growth factor-10 (FGF-10) and impairs epithelial–mesenchymal interactions during lung development; however, the mechanisms connecting inflammatory signaling with reduced growth factor expression are not yet understood. In this study we found that soluble inflammatory mediators present in tracheal fluid from preterm infants can prevent saccular airway branching. In addition, LPS treatment led to local production of mediators that inhibited airway branching and FGF-10 expression in LPS-resistant C.C3-*Tlr4*^{Lpsd}/J fetal mouse lung explants. Both direct NF-κB activation and inflammatory cytokines (IL-1β and TNF-α) that activate NF-κB reduced FGF-10 expression, whereas chemokines that signal via other inflammatory pathways had no effect. Mutational analysis of the FGF-10 promoter failed to identify genetic elements required for direct NF-κB–mediated FGF-10 inhibition. Instead, NF-κB activation appeared to interfere with the normal stimulation of FGF-10 expression by Sp1. Chromatin immunoprecipitation and nuclear

Address correspondence and reprint requests to Dr. Lawrence S. Prince, Division of Neonatology, Departments of Pediatrics and Cell and Developmental Biology, Vanderbilt University School of Medicine, 9435A MRBIV, 2213 Garland Avenue, Nashville, TN 37232. lawrence.s.prince@vanderbilt.edu.

[1]Current address: Division of Neonatology, Department of Pediatrics, University of South Alabama, Mobile, AL.

The online version of this article contains supplemental material.

Disclosures

The authors have no financial conflicts of interest.

coimmunoprecipitation studies demonstrated that the RelA subunit of NF-κB and Sp1 physically interact at the FGF-10 promoter. These findings indicate that inflammatory signaling through NF-κB disrupts the normal expression of FGF-10 in fetal lung mesenchyme by interfering with the transcriptional machinery critical for lung morphogenesis.

Epithelial–mesenchymal interactions guide lung development. Cells that arise from the foregut endoderm line the airways. These epithelial airways are surrounded by mesenchyme, which drives airway extension and branching. The lung bronchial tree forms first, followed by expansion and branching of more distal saccular airways (1-3). During branching morphogenesis, the fetal lung mesenchyme expresses multiple growth factors that act on airway epithelia. Fibroblast growth factor 10 (FGF-10) is among the key mesenchymal growth factors for lung development, promoting airway extension and branching (4, 5). During canalicular and saccular airway formation (beginning at embryonic day [E] 14 in mice, 22 wk gestation in humans), FGF-10 continues to stimulate airway branching. The terminal saccular airways will become alveolar ducts as the lung reaches maturity and alveolarization progresses (6).

Abnormalities in lung branching morphogenesis can lead to human disease. In up to 50% of extremely preterm infants, saccular airway branching arrests, resulting in bronchopulmonary dysplasia (BPD) (7, 8). Arrested branching in BPD results in fewer alveolar units available for gas exchange and smaller overall lung volumes (9). Although many factors likely contribute to BPD pathogenesis, exposure to inflammation clearly increases BPD risk. Infants exposed prenatally to chorioamnionitis (infection or inflammation of the amniotic membranes, uterus, or placenta) or postnatally to bacteremia and sepsis are more likely to develop BPD (10, 11). These clinical observations suggest that inflammatory mediators transmitted to the lungs might prevent normal canalicular and saccular stage lung development. The process by which inflammatory signaling disrupts normal developmental processes is not clear, but recent findings have provided clues to the mechanisms linking inflammation and BPD pathogenesis.

Activation of the innate immune system in fetal mice inhibits saccular stage lung development. Injecting Gram-negative bacterial LPS, a classic activator of innate immunity, into the amniotic fluid of mice at E15 causes cystic dilation of saccular airways and inhibits airway branching. LPS also acts in a TLR4-dependent manner to inhibit saccular airway branching in lung explants (12). In preventing normal morphogenesis, LPS inhibits expression of FGF-10, a key mesenchymal growth factor required for airway branching (13). Under normal conditions, the fetal lung mesenchyme is not continuously exposed to the external environment. Therefore, LPS and other bacterial constituents might not directly signal mesenchymal cells to inhibit FGF-10 expression and disrupt branching. Instead, innate immune activation may lead to local production of soluble inflammatory mediators that affect the lung mesenchyme. Although innate immune signaling appears to alter branching morphogenesis in part through reduced FGF-10 expression, several important questions remain unanswered, including the following: 1) What are the critical inflammatory mediators in the airways of premature infants at risk for BPD?; 2) what are the important downstream signaling pathways?; and 3) how do these pathways lead to reduced expression

of FGF-10 (and possibly other mediators) and impaired mesenchymal–epithelial interactions that block normal lung development? Identifying the connections between inflammatory signaling and lung morphogenesis is critical for understanding the disease mechanisms leading to BPD.

Because preterm infants are commonly exposed to an inflammatory environment immediately before birth, we tested whether the inflammatory milieu in the airways of newborn preterm infants contains substances that could inhibit lung development. We then measured the ability of soluble inflammatory mediators to alter FGF-10 expression in fetal lung mesenchyme and found that mediators that activate NF-κB signaling can inhibit FGF-10 expression. Investigation into the mechanism of FGF-10 inhibition by NF-κB revealed that NF-κB blocks FGF-10 expression by interfering with the ability of Sp1 to drive FGF-10 transcription. Interactions between NF-κB and Sp1 may provide a potential target for preserving FGF-10 expression during lung development, with implications for novel approaches to preventing or treating BPD in preterm infants.

Materials and Methods

Reagents and cell culture

Phenol-extracted, gel-purified *Escherichia coli* LPS (O55:B5) was purchased from Sigma-Aldrich (St. Louis, MO). Recombinant IL-1β, TNF-α, MIP-1α, and MCP-1 were purchased from R&D Systems (Minneapolis, MN). Parthenolide, the IκB kinase β (IKKβ) inhibitor BMS345541, and the MAPK inhibitors PD98059, SB203580, U0126, FPTIII, and ZM336372 were purchased form EMD Biosciences (San Diego, CA). Abs against RelA and Sp1 were obtained from Santa Cruz Biotechnology (Santa Cruz, CA). Rat anti–E-cadherin was purchased from Zymed (San Francisco, CA). Alexa-conjugated secondary Abs were obtained from Invitrogen (Carlsbad, CA).

Animals and saccular explant culture

BALB/cJ and C.C3-*Tlr4*^{Lpsd}/J mice were obtained from The Jackson Laboratory (Bar Harbor, ME). For timed matings, the morning of vaginal plug discovery was defined at E0. Our procedure for culturing saccular stage fetal lung explants has been described (13-15). Briefly, E15 mice were euthanized and the fetal mouse lungs dissected free of surrounding structures. The lung tissue was minced into 0.5-1 mm^3 cubes and cultured on an air–liquid interface using permeable supports (Costar Transwell; Corning, Corning, NY) and serum-free DMEM. Explants were cultured at 37°C in 95% air/5% CO_2 for up to 72 h. To isolate conditioned media from BALB/cJ explants, LPS was included in culture media at a concentration of 250 ng/ml. After 72 h of culture, the media were removed and stored at -80°C. Conditioned media from control and LPS-treated BALB/cJ explants were then added to freshly isolated C.C3-*Tlr4*^{Lpsd}/J explants.

Immunostaining, imaging, and analysis

To quantify saccular airway branching in cultured lung explants, brightfield images of explants were acquired following 24 h and 72 h of culture. The explant area and number of saccular airways along the periphery of each explant were measured with the assistance of

the Image Processing Toolkit (Reindeer Graphics, Asheville, NC) within Photoshop (Adobe, San Jose, CA). Airway branching was then expressed as the number of new branches per square millimeter that formed between 24 and 72 h of culture in each explant. For immunostaining of Sp1 and E-cadherin in fetal mouse lungs, E16 BALB/cJ mouse lungs were dissected, rinsed in PBS, and processed in increasing sucrose concentrations. Lungs were then frozen in OCT and stored at −80°C. Cryostat sections (8 μm) were fixed with 4% paraformaldehyde, permeabilized with 0.1% Triton X-100, and stained with Abs against Sp1 and E-cadherin. Alexa-conjugated secondary Abs were used for fluorescent detection, and nuclei were labeled with DAPI. Images were acquired using an Olympus FV1000 laser scanning confocal microscope (Olympus, Melville, NY).

Tracheal aspirate collection and cytokine measurement

Tracheal aspirate samples were obtained from intubated preterm infants. All protocols were reviewed and approved by the Institutional Review Board at the University of Alabama at Birmingham, Birmingham, AL. Eligible patients were delivered between 23 and 28 wk gestation and intubated on the first day of life. Tracheal aspirates were collected prior to 24 h of age. Endotracheal suctioning was performed using an enclosed inline suction catheter. Then 1 ml sterile saline was instilled into the endotracheal tube, and fluid was aspirated into an enclosed specimen trap. Following centrifugation at 2000 × *g* at 4°C for 5 min, the supernatant was filtered through a 0.45-μm low protein binding syringe filter (Millipore, Bedford, MA), aliquoted, and stored at −80°C. Urea concentration in each aspirate was measured using the Quantichrom Urea Assay kit (Bioassay Systems, Hayward, CA). Samples were diluted to a final urea concentration of 0.1 mg/dl before use. Patient identifiers were not obtained, but presence or absence of maternal chorioamnionitis was recorded. All cases of chorioamnionitis were confirmed by placental pathologic examination. Cytokine concentrations in each sample were measured by SearchLight Assay (Pierce Endogen/Thermo Fisher Scientific, Rockford, IL). Each sample was measured in triplicate over multiple dilutions.

RNA isolation, reverse transcription, and real-time PCR

Total RNA was isolated from fetal lung explants and cultured mesenchyme, using TRIzol reagent (Invitrogen) and standard protocols. Three explants were pooled for each sample. First-strand cDNA was synthesized using oligo-dT primers and MMLV reverse transcriptase (SuperScript II; Invitrogen). PCR primers designed using Beacon Designer software (Bio-Rad, Hercules, CA) were validated by performing electrophoresis and melting temperature analysis of the PCR product. Standard concentration curves were done for each primer pair used. Two-step real-time PCR was performed with a Bio-Rad MyiQ thermocycler and SYBR Green detection (Bio-Rad). We normalized gene expression to GAPDH in each sample. The $2^{-\Delta\Delta CT}$ method was used to compare gene expression levels between samples (16). Independent experiments were performed at least three separate times. Data between groups were compared by ANOVA to test for significant differences.

Plasmids

The FGF-10 luciferase reporter in the pXPI vector was generously supplied by Benoit Bruneau (Gladstone Institute of Cardiovascular Disease, San Francisco, CA) (17). This construct contains an ~6-kb *Bam*HI fragment from the murine FGF-10 gene placed immediately upstream of the luciferase coding sequence. Serial truncations of the FGF-10 promoter were generated by PCR mutagenesis. Deletions were confirmed by restriction digest and sequencing. The predicted NF-κB binding site in the FGF-10 promoter located 555 bp upstream of the start site was deleted from the 0.9-kb FGF-10-D truncation, using site-directed mutagenesis. Primers compatible with the QuikChange II mutagenesis system (Agilent, Palo Alto, CA) were synthesized (5′-CTT CCC CCC TCC CTG TTC CCA GCA GCT T-3′; 5′-AAG CTG CTG GGA ACA GGG AGG GGG GAA G-3′). Positive transformants were sequenced to ensure deletion. FGF-10 luciferase reporter constructs were cotransfected into Chinese hamster ovary (CHO) cells, using SuperFect lipofection reagent (Qiagen, Valencia, CA). pSV-β-Gal was included to control for transfection efficiency. After 48 h, cells were lysed and luciferase activity was measured with Steady-Glo reagent (Promega, Madison, WI) and a microtiter plate luminometer. Light units were normalized to β-galactosidase levels.

Constitutively active IKKβ and dominant-negative IκB cDNA constructs (18) were cloned into pCDNA3.1/CT-GFP for expression in CHO cells. Murine Sp1 was cloned from E15 fetal mouse lung RNA by reverse transcription and PCR, using the following primers: 5′-GCC ACC ATG AGC GAC CAA GAT CAC TCC A-3′; 5′-GGA AAC CAT TGC CAC TGA TAT T-3′. The full-length Sp1 sequence was first subcloned into pCR2.0, sequenced, excised by restriction digestion, and ligated into pCDNA3.1/CT-GFP for expression.

Coimmunoprecipitation

For coimmunoprecipitation of Sp1 and p65, CHO cells were lysed with icecold hypotonic lysis buffer (10 mM HEPES pH 7.6, 1 mM EDTA, 60 mM KCl, 0.5% Nonidet P-40, 1 mM DTT, and protease inhibitors [Halts, Pierce, Rockford, IL]). Lysates were centrifuged for 10 min at 16,000 × *g* (4°C) for separation of nuclear pellet from cytoplasmic supernant. The nuclear fraction was resuspended in 250 mM Tris-HCl pH 7.8, 1 mM DTT, and protease inhibitors and frozen at −80°C. Samples were then thawed and diluted with nuclear dilution buffer (0.01% SDS, 1.1% Triton X-100, 1.2 mM EDTA, 16.7 mM Tris-HCl pH 8.0, and 167 mM NaCl). Nuclear and cytoplasmic fractions were precleared with Protein G agarose beads (Sigma-Aldrich) and immunoprecipitated overnight. After washing, immunoprecipitates were boiled in Laemmli sample buffer, separated by SDS-PAGE, and transferred to polyvinylidene difluoride membranes. Blots were blocked with 5% nonfat dry milk with 0.05% Tween-20, probed with anti-RelA Abs, and developed by chemiluminescence.

Chromatin immunoprecipitation

Chromatin immunoprecipitation was performed using primary fetal mouse lung mesenchymal cells. Control and LPS-treated cells were fixed with 1% formaldehyde and lysed. DNA was sheared by sonication, phenol:chloroform extracted, and precipitated with ethanol. Samples were then incubated with anti-Sp1 and anti-p65 Abs for immunoprecipitation. Following stringent washing, DNA–protein linkages were disrupted

and released DNA fragments were phenol:chloroform extracted and precipitated with ethanol. The 320-bp region of the FGF-10 promoter (upstream of and including the transcriptional start site) was detected by PCR. Products were analyzed by agarose gel electrophoresis.

Results

Inflammatory mediators in newborn lungs inhibit airway branching

To investigate whether the inflammatory milieu in the airways of newborn preterm infants contains substances that could inhibit lung development, we tested patient samples using an experimental model of saccular lung development. We isolated tracheal aspirate fluid from 22 newborn extremely preterm infants divided into three distinct groups. Nine infants were exposed to maternal chorioamnionitis, seven infants were born preterm owng to maternal preeclampsia, and six infants were delivered preterm without an identifiable cause and without clinical or pathological evidence of chorioamnionitis. Each tracheal aspirate sample was separately added to E15 BALB/cJ fetal mouse lung explants to measure effects on saccular airway branching and FGF-10 expression. As shown in Fig. 1, samples from infants exposed to chorioamnionitis significantly inhibited the formation of new saccular airway branches in explants, compared with pre-eclampsia and control preterm labor samples. Representative images in Fig. 1 show that tracheal aspirate fluid from infants exposed to chorioamnionitis caused formation of more cystic, poorly branched airways (Fig. 1*C*, 1*F*). In contrast, tracheal aspirate fluid from infants delivered preterm owing to maternal pre-eclampsia had no effect on saccular airway branching or formation (Fig. 1*B*, 1*E*). New saccular airway branches were significantly reduced in explants exposed to aspirates from the chorioamnionitis samples compared with control explants grown in media alone or with tracheal aspirates from the other patient groups (Fig. 1*G*). Tracheal aspirates from patients exposed to chorioamnionitis also contained elevated levels of inflammatory cytokines, compared with those from infants born preterm owing to maternal pre-eclampsia or undiagnosed causes (Fig. 1*H*, Supplemental Table I). LPS was not detected in any of the tracheal aspirate samples tested (<0.1 EU/ml). Together, these data suggest that soluble inflammatory mediators in the airway of infants exposed to chorioamnionitis can inhibit saccular airway morphogenesis.

Because data from patient samples suggested that soluble mediators could inhibit saccular airway branching, we asked whether these mediators are produced locally in fetal lungs. To address this issue, we collected LPS-conditioned media from BALB/cJ fetal mouse lung explants. LPS stimulated the release of multiple inflammatory mediators into the media (Supplemental Fig. 1). We then added the LPS-conditioned media to explants from C.3-*Tlr4*^{Lpsd}/J mice, which are resistant to the direct effects of LPS owing to a loss of function mutation in TLR4. LPS-conditioned media from BALB/cJ explants substantially inhibited saccular airway branching in C.C3-*Tlr4*^{Lpsd}/J explants (Fig. 2*A*–*G*) and reduced FGF-10 expression (Fig. 2*H*). These effects were reduced when the NF-κB inhibitor parthenolide was included in the media (Fig. 2*C*, 2*F*). Together, these data indicate that soluble inflammatory mediators produced in the lungs can inhibit FGF-10 expression and saccular airway branching, possibly through NF-κB signaling.

Inflammatory mediators downregulate FGF-10 expression through the NF-κB pathway

To better understand which cytokines and pathways might regulate FGF-10 expression, we treated primary fetal mouse lung mesenchyme with LPS or individual cytokines and chemokines. IL-1β and TNF-α, which activate NF-κB, inhibited FGF-10 expression, whereas the CC chemokines MCP-1 and MIP1α had no effect (Fig. 3*A*). LPS, IL-1β, and TNF-α each inhibited FGF-10 expression within 4 h of treatment, and this reduction in gene expression persisted for up to 48 h (Fig. 3*B*).

Because several lines of investigation suggested that NF-κB signaling was involved in the reduction of airway branching and FGF-10 expression by inflammatory mediators, we asked whether the NF-κB pathway might directly inhibit FGF-10 expression. For these studies, we used an FGF-10 luciferase reporter construct in transfected CHO cells. As shown in Fig. 3*C*, both IL-1β and TNF-α inhibited FGF-10 promoter activity as measured by luciferase activity. In these cultured cells, parthenolide could not completely block the effects of IL-1β, but the more specific IKKβ inhibitor BMS345541 did prevent the decrease in FGF-10 luciferase expression with IL-1β or TNF-α. We next used a molecular approach to further test if direct activation or inhibition of NF-κB, in the absence of inflammatory mediators, could alter FGF-10 expression. Cotransfection of CHO cells with a constitutively active IKKβ mutant (caIKK) (18) with the FGF-10 luciferase reporter construct inhibited FGF-10 promoter activity (Fig. 3*D*). We then used a dominant-negative IκB mutant to block NF-κB activity (18). Cotransfection of the dominant-negative IκB mutant increased FGF-10 luciferase expression, indicating baseline regulation of FGF-10 by NF-κB in the absence of inflammatory stimuli. To verify that these effects were not due to MAPK activation, we used chemical inhibitors of various MAPK targets to test if they affected FGF-10 expression. As seen in Fig. 3*E*, IL-1β inhibited FGF-10 luciferase activity in the presence of each inhibitor, suggesting that MAPK activity was not required to inhibit FGF-10 expression.

Sp1 and NF-κB interactions regulate FGF-10 transcription

Analysis of the FGF-10 promoter sequence revealed multiple predicted NF-κB binding sites within 5.9 kb of the transcriptional start site (Fig. 4*A*). To determine whether these sites are required for inhibition of FGF-10 by NF-κB, serial truncations of the FGF-10 promoter were expressed in CHO cells. As seen in Fig. 4*B* and 4*C*, IL-1β and caIKKβ inhibited activity of all of the truncated promoters, even the shortest construct (FGF-10-D) containing 350 bp upstream of the start site and only a single predicted NF-κB binding site. Deletion of this predicted NF-κB binding site did not prevent inhibition by caIKKβ (Fig. 4*D*), suggesting that NF-κB may inhibit FGF-10 expression via interaction with other factors. The FGF-10 promoter region contains multiple guanosine-cytosine boxes (GC boxes), which are predicted to bind Sp1 family transcription factors (19, 20). Interestingly, Sp1 expression was heterogeneous in developing fetal mouse lung, with mesenchymal cells adjacent to branching airways having variable levels of Sp1 expression (Fig. 5*B*). Transfecting Sp1 increased FGF-10 reporter activity in a concentration-dependent manner (Fig. 5*C*). These data, along with the multiple GC boxes in the FGF-10 promoter, suggest that Sp1 may be an important stimulator of FGF-10 expression in the fetal lung mesenchyme.

As Sp1 was expressed in fetal lung mesenchyme and stimulated FGF-10 expression, we next tested whether NF-κB activation might interfere with Sp1-mediated FGF-10 transcription. Cotransfection of either the RelA component of NF-κB or caIKKβ inhibited the ability of Sp1 to drive FGF-10 expression, suggesting a negative interaction between Sp1 and NF-κB on the FGF-10 promoter (Fig. 5*D*). We further investigated potential Sp1 and RelA interaction, using chromatin immunoprecipitation. Primary fetal lung mesenchymal cells were isolated, cultured, and treated with LPS. Crosslinked DNA was sheared into 300- to 500-bp fragments, and protein–DNA complexes were immunoprecipitated using Abs against Sp1 and RelA. We measured binding of Sp1 and RelA to the FGF-10 promoter, using PCR primers flanking a 320-bp region immediately upstream of the transcriptional start site. In control cells, FGF-10 DNA was detected in Sp1 immunoprecipitates but was barely detectable in RelA samples (Fig. 5*E*). LPS treatment stimulated interaction between the FGF-10 promoter and both Sp1 and RelA. In addition to this chromatin immunoprecipitation data, RelA and Sp1 were coimmunoprecipitated from CHO cells, further demonstrating protein–protein interaction (Fig. 5*F*). Collectively, these data indicate that RelA and Sp1 interact at the FGF-10 promoter, and that NF-κB may prevent Sp1-mediated FGF-10 expression.

Discussion

In preterm infants, inflammation arrests saccular airway formation, leading to BPD (9, 21). Identifying how inflammation alters the epithelial–mesenchymal interactions critical for lung development is important for understanding BPD pathogenesis. We show in this paper that NF-κB activation inhibits expression of FGF-10, a key growth factor for lung development. Both LPS and soluble inflammatory mediators that signal through the NF-κB pathway can decrease FGF-10 in the fetal lung mesenchyme and in heterologous reporter systems. Interestingly, these effects do not appear to require direct DNA binding of NF-κB to a canonical NF-κB response element in the FGF-10 promoter. Instead, our data suggest that NF-κB interacts with Sp1 at the FGF-10 promoter, inhibiting the ability of Sp1 to drive FGF-10 expression. The ability of NF-κB to disrupt normal Sp-1 mediated expression during development may link inflammation and altered lung morphogenesis at the molecular level.

A variety of microbial pathogens can cause chorioamnionitis and neonatal sepsis (22, 23). The risk of developing BPD following exposure to infection or inflammation is not exclusive to a particular pathogen. Many different microorganisms and microbial products activate NF-κB (24), making this a common mechanism by which infection and inflammation can inhibit normal lung development. In addition, injurious stimuli, such as hyperoxia, may release soluble mediators that can the activate NF-κB within the lung (25). The cellular site of NF-κB activation may also play an important role in BPD pathogenesis. Our data show that inflammation and NF-κB activation can alter the expression of genes in the fetal lung mesenchyme in disease. As these cells are critical for airway development, they may be key targets of inflammation. In gaining access to and targeting the fetal lung mesenchyme, microbial products and TLR agonists must breach the barriers provided by the airway epithelia or pulmonary vascular endothelia to directly activate NF-κB and inhibit FGF-10 in the interstitially located mesenchymal cells. Alternatively, the initial cellular site

of inflammatory response may be the airway epithelia or lung macrophage. These activated cells may then release soluble inflammatory mediators, including TNF-α and IL-1β, that then activate NF-κB in fetal lung mesenchyme, inhibiting FGF-10 and preventing airway branching. By either path, NF-κB activation in fetal lung mesenchymal cells appears to be a key mechanism in arresting lung morphogenesis.

During the innate immune response, NF-κB stimulates expression of many proinflammatory genes. This pathway linking microbial products and cytokines to increased gene expression has been well studied (26). In the absence of inflammatory stimuli, NF-κB subunits are bound to IκB in the cell cytoplasm, where they remain quiescent. Activation of innate immune signaling via microbial substances or cytokines increases IKK activity, leading to phosphorylation and degradation of IκB and releasing NF-κB to traffic into the nucleus. The termination of NF-κB activation can occur by displacing the NF-κB complex from genomic DNA or by targeted degradation of nuclear NF-κB proteins. The mechanisms linking NF-κB to suppression of gene expression, however, are not as well understood. Many of the genes activated by NF-κB are proinflammatory cytokines or contribute to the cellular inflammatory response. Genes downregulated by NF-κB are less numerous, are involved in more diverse cellular roles, and do not have obvious connections to the inflammatory response (27, 28). Because of NF-κB's transactivation function when bound to DNA, inhibition of gene expression may involve protein–protein interactions in which NF-κB subunits prevent binding or activation of other stimulatory transcription factors, resulting in decreased gene expression. Interestingly, NF-κB appears to interfere with Sp1-mediated transcription in several genes, including BMP4 (29), TGFBRII (30), and the collagen genes Col1A2 (31) and Col2A1 (32). Although genes inhibited by Sp1–NF-κB interaction may play similar roles in tissue morphogenesis and wound healing, a more genome-wide assessment is required before determining the significance of this mechanism.

Our data suggest that NF-κB inhibits the normal stimulatory function of Sp1 in FGF-10 expression. Sp1 strongly activates FGF-10 expression, likely through binding the multiple GC boxes present in the FGF-10 promoter. Increasing Sp1 concentrations often amplify the expression of genes like FGF-10 with arrays of GC boxes. Amplification appears to involve both Sp1–DNA binding and the formation of large tertiary Sp1–Sp1 complexes that function to recruit components of the basal transcriptional apparatus (33). NF-κB and Sp1 interactions can both promote and inhibit transcriptional activation. NF-κB and Sp1 cooperate to increase HIV-1 transcription by binding distinct but immediately adjacent DNA sequences (34). Sp1 binds consensus NF-κB sequences in the P-selectin (35), NR1 (36), and IL-6 promoters (37), competing with RelA for DNA binding. Sp1 and RelA also interact at the protein–protein level (38), as we also demonstrated in CHO cells. We speculate that RelA may prevent Sp1-mediated amplification and tertiary Sp1–Sp1 complex formation on the FGF-10 promoter. NF-κB activation may also recruit additional inhibitory transcription factors to the FGF-10 promoter, reducing gene expression. The Sp family member Sp3 can act as an inhibitor of Sp1-mediated gene amplification, binding GC boxes but preventing Sp1–Sp1 complex formation (39, 40). Our future studies will further test these potential mechanisms for regulating FGF-10 expression. The findings presented in this paper also raise the possibility that NF-κB activation could cause a change in mesenchymal cell differentiation. Instead of expressing critical growth factors or other genes important for

fetal lung morphogenesis, mesenchymal cells exposed to inflammation may adopt a more mature fibroblast-like phenotype. Although these cells would normally be found in fully developed tissues, they could lack the ability to drive airway morphogenesis in an immature lung.

Understanding how inflammation disrupts normal morphogenesis will help identify the molecular mechanisms of developmental disorders. Our data show that many soluble inflammatory mediators are produced locally in the fetal and neonatal lung following exposure to microbial products, but only certain mediators appear to inhibit growth factor expression. Inflammatory cytokines that activate the IKKβ/NF-κB pathway in lung mesenchymal cells inhibit FGF-10 expression and therefore likely disrupt epithelial–mesenchymal interactions during airway branching. Apart from its well-described role in stimulating the innate immune response, NF-κB activation in the lung mesenchyme cells interferes with Sp1-mediated FGF-10 expression. Because Sp1 regulates expression of many genes, NF-κB activation may have widespread effects on the normal developmental program. Future studies will need to clarify if these changes are fully reversible or if they cause lasting changes in the developing lung. Better understanding of these alterations could define new therapeutic targets for preventing or treating morbidities associated with preterm birth.

Supplementary Material

Refer to Web version on PubMed Central for supplementary material.

Acknowledgments

We thank Brian Halloran, Lily Zhang, and Amanda Stinnett for technical assistance and William W. Andrews and Dee Dee Lyon for help in measuring inflammatory markers.

This work was supported by the American Lung Association (to L.S.P); the March of Dimes (to L.S.P.); National Institutes of Health Grants HL-086324 (to L.S.P), HL-097195 (to L.S.P. and T.S.B.), and AI-079253 (to T.S.B); the Department of Veterans Affairs (to T.S.B.); Neonatal Research Fellowships from Ikaria (to J.T.B., J.D.M., and E.J.P.) and Discovery Laboratories (to J.D.M.); and a National Institute of Child Health and Human Development T32 Fellowship (to E.J.P.). Confocal imaging was performed through the use of the Vanderbilt University Medical Center Cell Imaging Shared Resource (supported by National Institutes of Health Grants CA68485, DK20593, DK58404, HD15052, DK59637, and EY08126).

References

1. Warburton D, Schwarz M, Tefft D, Flores-Delgado G, Anderson KD, Cardoso WV. The molecular basis of lung morphogenesis. Mech Dev. 2000; 92:55–81. [PubMed: 10704888]
2. Perl AK, Whitsett JA. Molecular mechanisms controlling lung morphogenesis. Clin Genet. 1999; 56:14–27. [PubMed: 10466413]
3. Hogan BL, Yingling JM. Epithelial/mesenchymal interactions and branching morphogenesis of the lung. Curr Opin Genet Dev. 1998; 8:481–486. [PubMed: 9729726]
4. Weaver M, Batts L, Hogan BL. Tissue interactions pattern the mesenchyme of the embryonic mouse lung. Dev Biol. 2003; 258:169–184. [PubMed: 12781691]
5. Weaver M, Dunn NR, Hogan BL. Bmp4 and Fgf10 play opposing roles during lung bud morphogenesis. Development. 2000; 127:2695–2704. [PubMed: 10821767]
6. Hokuto I, Perl AK, Whitsett JA. Prenatal, but not postnatal, inhibition of fibroblast growth factor receptor signaling causes emphysema. J Biol Chem. 2003; 278:415–421. [PubMed: 12399466]

7. Christou H, Brodsky D. Lung injury and bronchopulmonary dysplasia in newborn infants. J Intensive Care Med. 2005; 20:76–87. [PubMed: 15855220]
8. MacDorman MF, Martin JA, Matthews TJ, Hoyert DL, Ventura SJ. Explaining the 2001-2002 infant mortality increase: data from the linked birth/infant death data set. Natl Vital Stat Rep. 2005; 53:1–22. [PubMed: 15712582]
9. May C, Prendergast M, Salman S, Rafferty GF, Greenough A. Chest radiograph thoracic areas and lung volumes in infants developing bronchopulmonary dysplasia. Pediatr Pulmonol. 2009; 44:80–85. [PubMed: 19085927]
10. Watterberg KL, Demers LM, Scott SM, Murphy S. Chorioamnionitis and early lung inflammation in infants in whom bronchopulmonary dysplasia develops. Pediatrics. 1996; 97:210–215. [PubMed: 8584379]
11. Klinger G, Levy I, Sirota L, Boyko V, Lerner-Geva L, Reichman B. collaboration with the Israel Neonatal Network. Outcome of early-onset sepsis in a national cohort of very low birth weight infants. Pediatrics. 2010; 125:e736–e740. [PubMed: 20231184]
12. Prince LS, Dieperink HI, Okoh VO, Fierro-Perez GA, Lallone RL. Toll-like receptor signaling inhibits structural development of the distal fetal mouse lung. Dev Dyn. 2005; 233:553–561. [PubMed: 15830384]
13. Benjamin JT, Smith RJ, Halloran BA, Day TJ, Kelly DR, Prince LS. FGF-10 is decreased in bronchopulmonary dysplasia and suppressed by Toll-like receptor activation. Am J Physiol Lung Cell Mol Physiol. 2007; 292:L550–L558. [PubMed: 17071719]
14. Dieperink HI, Blackwell TS, Prince LS. Hyperoxia and apoptosis in developing mouse lung mesenchyme. Pediatr Res. 2006; 59:185–190. [PubMed: 16439576]
15. Prince LS, Okoh VO, Moninger TO, Matalon S. Lipopolysaccharide increases alveolar type II cell number in fetal mouse lungs through Toll-like receptor 4 and NF-kappaB. Am J Physiol Lung Cell Mol Physiol. 2004; 287:L999–L1006. [PubMed: 15475494]
16. Arocho A, Chen B, Ladanyi M, Pan Q. Validation of the 2- DeltaDeltaCt calculation as an alternate method of data analysis for quantitative PCR of BCR-ABL P210 transcripts. Diagn Mol Pathol. 2006; 15:56–61. [PubMed: 16531770]
17. Agarwal P, Wylie JN, Galceran J, Arkhitko O, Li C, Deng C, Grosschedl R, Bruneau BG. Tbx5 is essential for forelimb bud initiation following patterning of the limb field in the mouse embryo. Development. 2003; 130:623–633. [PubMed: 12490567]
18. Cheng DS, Han W, Chen SM, Sherrill TP, Chont M, Park GY, Sheller JR, Polosukhin VV, Christman JW, Yull FE, Blackwell TS. Airway epithelium controls lung inflammation and injury through the NF-kappa B pathway. J Immunol. 2007; 178:6504–6513. [PubMed: 17475880]
19. Briggs MR, Kadonaga JT, Bell SP, Tjian R. Purification and biochemical characterization of the promoter-specific transcription factor, Sp1. Science (New York, N Y). 1986; 234:47–52.
20. Wierstra I. Sp1: emerging roles—beyond constitutive activation of TATAless housekeeping genes. Biochem Biophys Res Commun. 2008; 372:1–13. [PubMed: 18364237]
21. Jobe AJ. The new BPD: an arrest of lung development. Pediatr Res. 1999; 46:641–643. [PubMed: 10590017]
22. Klinger G, Levy I, Sirota L, Boyko V, Reichman B, Lerner-Geva L. Epidemiology and risk factors for early onset sepsis among very-lowbirthweight infants. Am J Obstet Gynecol. 2009; 201:38.e1–6. [PubMed: 19380122]
23. Garland SM, Ní Chuileannáin F, Satzke C, Robins-Browne R. Mechanisms, organisms and markers of infection in pregnancy. J Reprod Immunol. 2002; 57:169–183. [PubMed: 12385841]
24. Li Q, Verma IM. NF-kappaB regulation in the immune system. Nat Rev Immunol. 2002; 2:725–734. [PubMed: 12360211]
25. Johnson BH, Yi M, Masood A, Belcastro R, Li J, Shek S, Kantores C, Jankov RP, Tanswell AK. A critical role for the IL-1 receptor in lung injury induced in neonatal rats by 60% O2. Pediatr Res. 2009; 66:260–265. [PubMed: 19542903]
26. Ozato K, Tsujimura H, Tamura T. Toll-like receptor signaling and regulation of cytokine gene expression in the immune system. Biotechniques. 2002; 66–68(Suppl):70. 72 passim.
27. Campbell KJ, Rocha S, Perkins ND. Active repression of anti-apoptotic gene expression by RelA(p65) NF-kappa B. Mol Cell. 2004; 13:853–865. [PubMed: 15053878]

28. Sitcheran R, Cogswell PC, Baldwin AS Jr. NF-kappaB mediates inhibition of mesenchymal cell differentiation through a posttranscriptional gene silencing mechanism. Genes Dev. 2003; 17:2368–2373. [PubMed: 14522944]
29. Zhu NL, Li C, Huang HH, Sebald M, Londhe VA, Heisterkamp N, Warburton D, Bellusci S, Minoo P. TNF-alpha represses transcription of human Bone Morphogenetic Protein-4 in lung epithelial cells. Gene. 2007; 393:70–80. [PubMed: 17350185]
30. Baugé C, Beauchef G, Leclercq S, Kim SJ, Pujol JP, Galéra P, Boumédiene K. NFkappaB mediates IL-1beta-induced down-regulation of TbetaRII through the modulation of Sp3 expression. J Cell Mol Med. 2008; 12(5A):1754–1766. [PubMed: 18053089]
31. Verrecchia F, Wagner EF, Mauviel A. Distinct involvement of the Jun-N-terminal kinase and NF-kappaB pathways in the repression of the human COL1A2 gene by TNF-alpha. EMBO Rep. 2002; 3:1069–1074. [PubMed: 12393755]
32. Chadjichristos C, Ghayor C, Kypriotou M, Martin G, Renard E, Ala-Kokko L, Suske G, de Crombrugghe B, Pujol JP, Galéra P. Sp1 and Sp3 transcription factors mediate interleukin-1 beta down-regulation of human type II collagen gene expression in articular chondrocytes. J Biol Chem. 2003; 278:39762–39772. [PubMed: 12888570]
33. Courey AJ, Holtzman DA, Jackson SP, Tjian R. Synergistic activation by the glutamine-rich domains of human transcription factor Sp1. Cell. 1989; 59:827–836. [PubMed: 2512012]
34. Perkins ND, Agranoff AB, Pascal E, Nabel GJ. An interaction between the DNA-binding domains of RelA(p65) and Sp1 mediates human immunodeficiency virus gene activation. Mol Cell Biol. 1994; 14:6570–6583. [PubMed: 7935378]
35. Hirano F, Tanaka H, Hirano Y, Hiramoto M, Handa H, Makino I, Scheidereit C. Functional interference of Sp1 and NF-kappaB through the same DNA binding site. Mol Cell Biol. 1998; 18:1266–1274. [PubMed: 9488441]
36. Liu A, Hoffman PW, Lu W, Bai G. NF-kappaB site interacts with Sp factors and up-regulates the NR1 promoter during neuronal differentiation. J Biol Chem. 2004; 279:17449–17458. [PubMed: 14970236]
37. Kang SH, Brown DA, Kitajima I, Xu X, Heidenreich O, Gryaznov S, Nerenberg M. Binding and functional effects of transcriptional factor Sp1 on the murine interleukin-6 promotor. J Biol Chem. 1996; 271:7330–7335. [PubMed: 8631753]
38. Kuang PP, Berk JL, Rishikof DC, Foster JA, Humphries DE, Ricupero DA, Goldstein RH. NF-kappaB induced by IL-1beta inhibits elastin transcription and myofibroblast phenotype. Am J Physiol Cell Physiol. 2002; 283:C58–C65. [PubMed: 12055073]
39. Majello B, De Luca P, Lania L. Sp3 is a bifunctional transcription regulator with modular independent activation and repression domains. J Biol Chem. 1997; 272:4021–4026. [PubMed: 9020109]
40. Yu B, Datta PK, Bagchi S. Stability of the Sp3-DNA complex is promoter-specific: Sp3 efficiently competes with Sp1 for binding to promoters containing multiple Sp-sites. Nucleic Acids Res. 2003; 31:5368–5376. [PubMed: 12954773]

Abbreviations used in this paper

BPD	bronchopulmonary dysplasia
caIKK	constitutively active IKKβ mutant
CHO	Chinese hamster ovary
DN-IκB	dominant-negative isoform of IκB
E	embryonic
FGF-10	fibroblast growth factor-10
GC box	guanosine-cytosine box

IKKβ	IκB kinase β
IKK inh	IKK inhibitor
parth	parthenolide

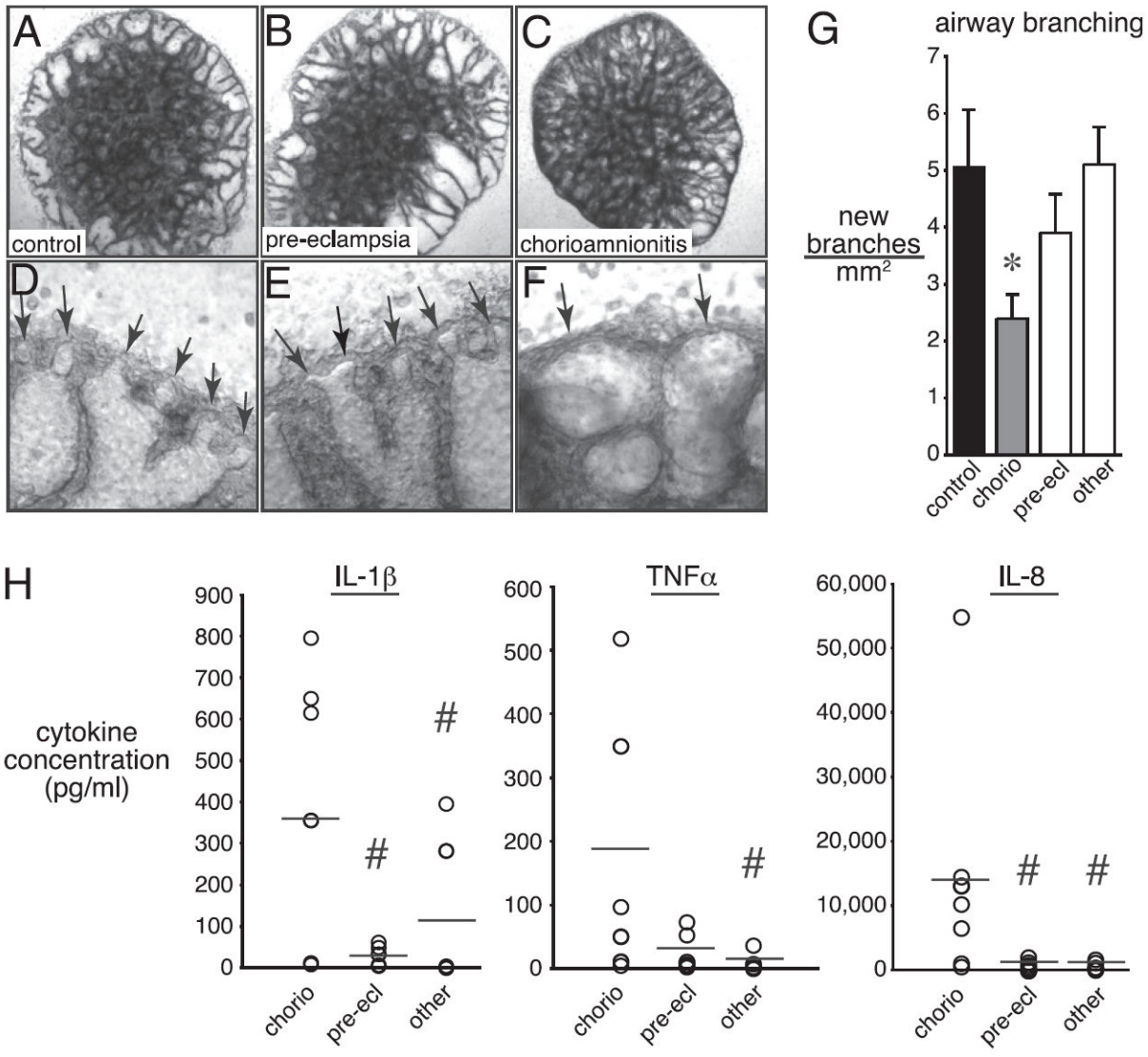

FIGURE 1.

Tracheal aspirate fluid from newborn patients exposed to chorioamnionitis inhibits airway branching. Tracheal fluid was aspirated from intubated extremely preterm infants following delivery and added to saccular stage fetal mouse lung explants. *A–F*, Brightfield images of control mouse lung explants (*A*, *D*) and explants cultured with tracheal aspirate fluid from a patient born preterm owing to maternal pre-eclampsia (*B*, *E*) or maternal chorioamnionitis (*C*, *F*) (original magnification ×25). Higher magnification images are shown in *D–F* (original magnification ×200). Arrows indicate saccular airways. *G*, The number of new saccular airway branches that formed during the culture period was lower when tracheal fluid from chorioamnionitis patients was added to the media. *$p < 0.05$; n = nine chorioamnionitis samples, seven pre-eclampsia samples, and six others. *H*, Concentrations of IL-1β, TNF-α, and IL-8 were measured in each patient sample. Elevated cytokine levels were detected in chorioamnionitis samples. Scale bar indicates mean concentration. #$p <$

0.05 compared with chorioamnionitis; *n* = nine chorioamnionitis samples, seven pre-eclampsia samples, and six others).

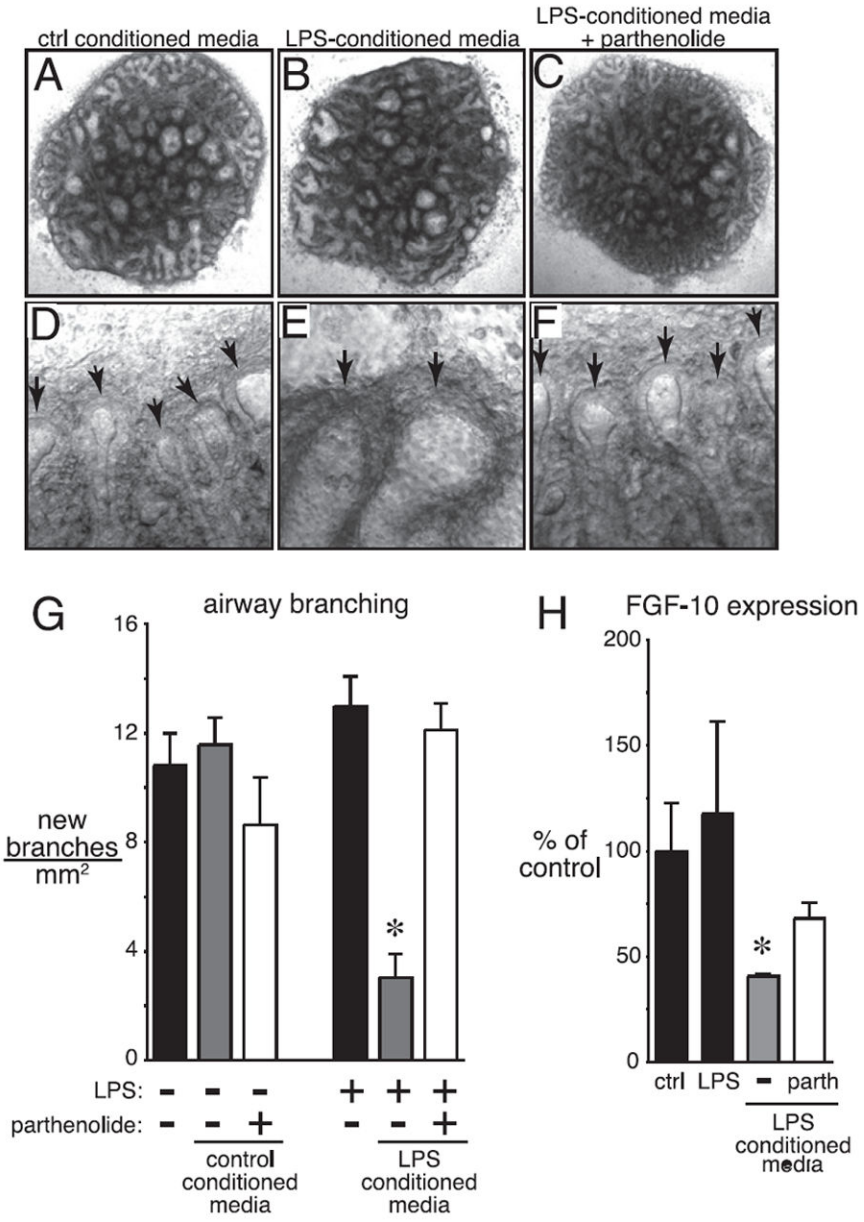

FIGURE 2.

LPS-conditioned media disrupt saccular airway branching in TLR4 mutant explants. Media from control and LPS-treated BALB/cJ explants were added to LPS-resistant C.C3-*Tlr4*^{Lpsd}/J explants. *A–F*, Brightfield images of C.C3-*Tlr4*^{Lpsd}/J explants cultured with control-conditioned media (*A, D*), LPS-conditioned media (*B, E*), or LPS-conditioned media with the NF-κB inhibitor parthenolide (1 μM; *C, F*) (original magnification ×25). Higher-magnification images are shown in *D–F* (original magnification ×200). Arrows indicate saccular airways. *G*, LPS-conditioned media inhibited formation of new saccular airways in C.C3-*Tlr4*^{Lpsd}/J explants. *$p < 0.001$; $n = 7$. *H*, LPS-conditioned media inhibited FGF-10 expression in C.C3-*Tlr4*^{Lpsd}/J explants, as measured by real-time PCR. *$p < 0.05$; $n = 9$.

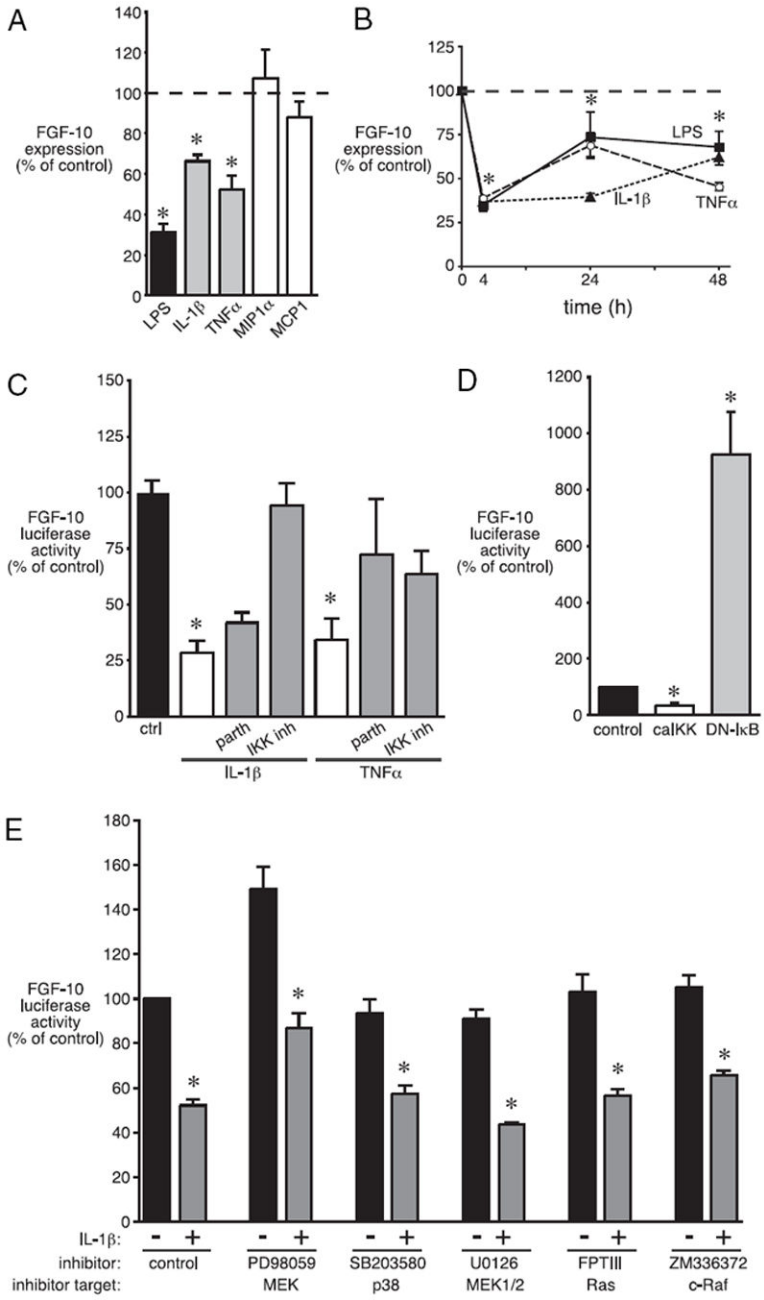

FIGURE 3.

NF-κB activation inhibits FGF-10 gene expression. *A*, Primary fetal mouse lung mesenchymal cells were treated with LPS (250 ng/ml), IL-1β (10 ng/ml), TNF-α (10 ng/ml), MIP-1α (100 ng/ml), or MCP-1 (100 ng/ml). Following 4 h of treatment, RNA was isolated and FGF-10 expression measured by real-time PCR. **p* < 0.05; *n* = 12. *B*, Time course of changes in FGF-10 gene expression following treatment of primary fetal mouse lung mesenchymal cells with LPS (solid line), TNF-α (dashed line), or IL-1β (dotted line). **p* < 0.05; *n* = 4 for IL-1β and TNF-α, *n* = 30 for LPS. *C*, IL-1β and TNF-α inhibit FGF-10 reporter activity. CHO cells transfected with FGF-10 luciferase were treated with IL-1β or

TNF-α in the absence (white bars) or presence (gray bars) of parthenolide (10 μm) or the IKKβ inhibitor BMS-345541 (1 μM). *$p < 0.05$; $n = 6$. *D*, Overexpression of caIKK inhibited FGF-10 reporter activity (white bar). Expressing a dominantnegative isoform of IκB increased FGF-10 reporter activity (gray bar). *$p < 0.05$; $n = 6$. *E*, Chemical MAPK inhibitors did not prevent IL-1β–mediated inhibition of FGF-10 reporter activity. *$p < 0.05$; $n = 6$. DN-IκB, dominant-negative isoform of IκB; IKK inh, IKK inhibitor; parth, parthenolide.

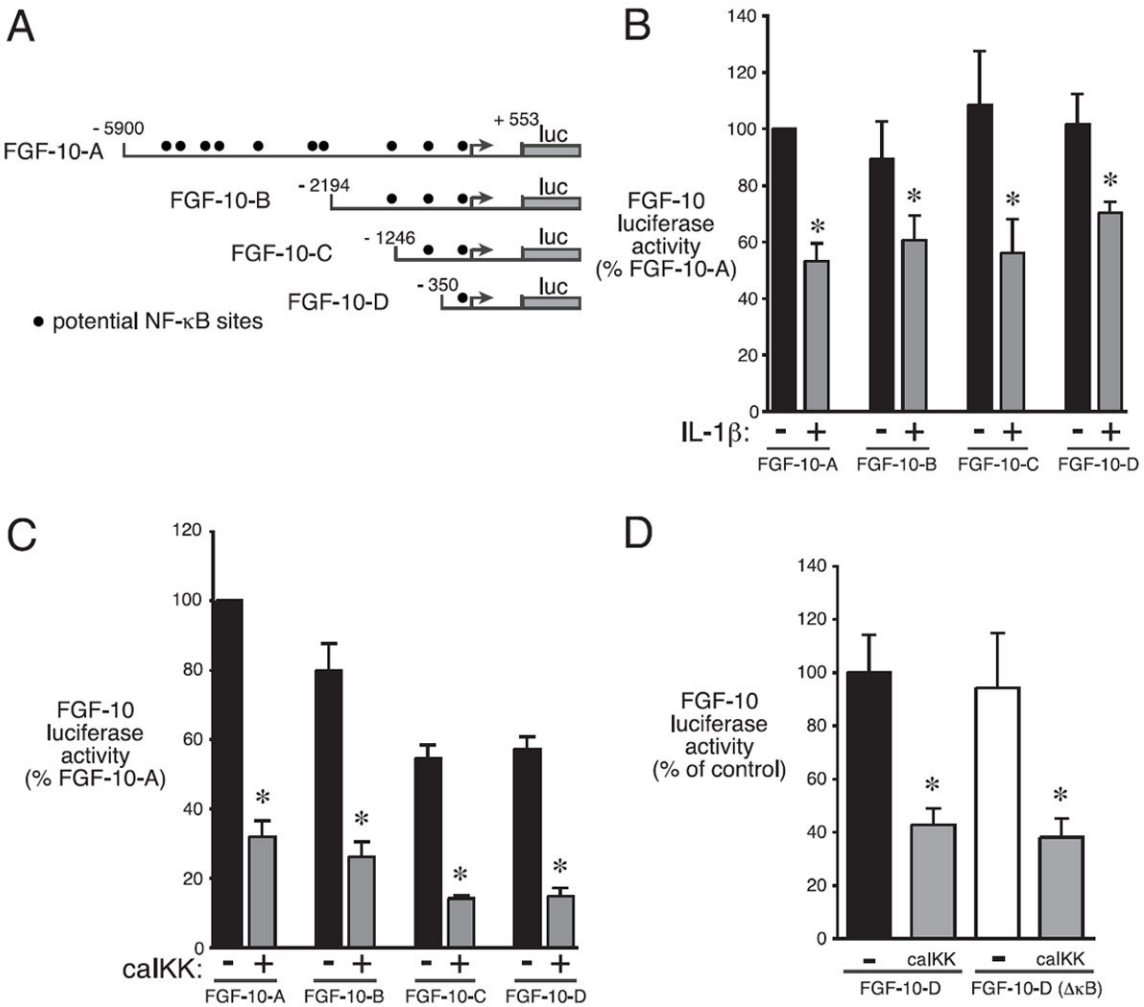

FIGURE 4.

NF-κB inhibits FGF-10 promoter activity via a noncanonical interaction near the FGF-10 transcriptional start site. *A*, Schematic diagram showing predicted NF-κB binding sites (●) along the FGF-10 promoter. Serial truncations of the FGF-10 promoter were generated as indicated. The FGF-10-D construct contained only a single predicted NF-κB binding site. *B* and *C*, Deletion of all but a 350-kb upstream region of the FGF-10 promoter retained sequences required for inhibition by IL-1β (*B*) or calKK (*C*). **p* < 0.05; *n* = 4. *D*, Deletion of the predicted NF-κB binding site in the FGF-10-D construct (ΔκB) did not prevent inhibition by caIKK. **p* < 0.05; *n* = 5.

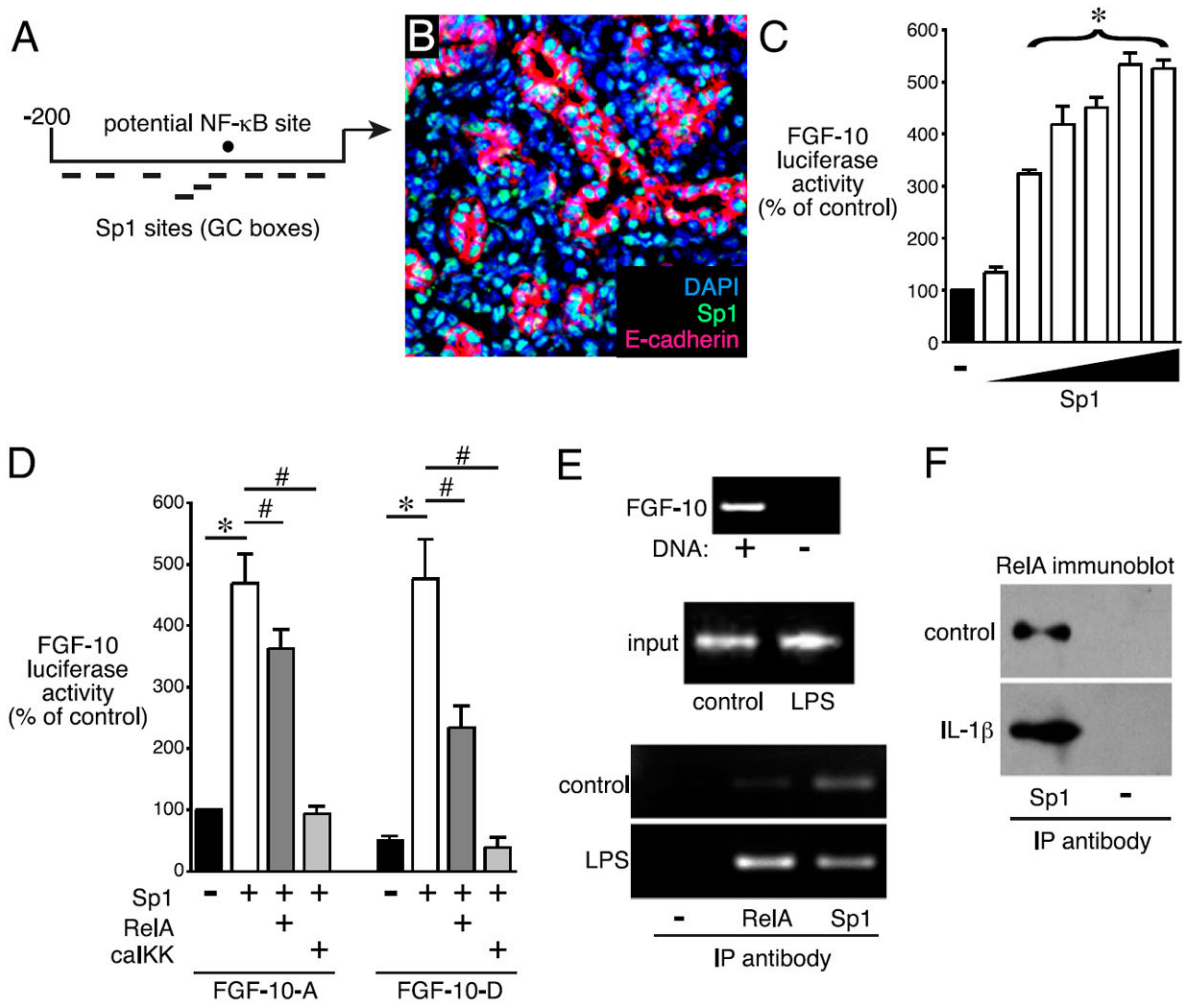

FIGURE 5.

NF-κB activation interferes with Sp1-mediated FGF-10 expression. *A*, Schematic diagram showing location of GC boxes predicted to bind Sp1 (black boxes) in relation to the predicted NF-κB binding site (●) and transcriptional start site in the FGF-10 promoter. *B*, Sp1 immunolocalization in fetal mouse lung. Cells within E16 fetal lung mesenchyme showed variable expression of Sp1 (green). Airway epithelia indicated by E-cadherin staining (red). Nuclei labeled with DAPI (blue) (original magnification ×400). *C*, Sp1 increased FGF-10 reporter activity. Increasing amounts of Sp1 cDNA were cotransfected into CHO cells along with the FGF-10 luciferase reporter. *$p < 0.05$; $n = 4$. *D*, NF-κB prevents Sp1-mediated FGF-10 expression. CHO cells were cotransfected with FGF-10 luciferase, Sp1 (white bars), and either RelA (dark gray bars) or caIKK (light gray bars). Experiments were repeated with the FGF-10-D truncated promoter with similar results (right side of graph). *$p < 0.05$; $n = 6$. *E*, LPS increases recruitment of RelA to the FGF-10 promoter. Primary fetal mouse lung mesenchymal cells were treated with LPS, and transcription factor binding to the FGF-10 promoter was measured by chromatin immunoprecipitation. A small amount of RelA–FGF-10 interaction was detected in control cells, with increased signal in LPS-treated cells. Sp1 appears to bind the FGF-10 promoter

both in control and in LPS-treated samples. *E*, Sp1 and RelA interact by coimmunoprecipitation. Sp1 was immunoprecipitated from control and IL-1β–treated CHO cell nuclear lysates. Samples were immunoblotted with Abs against RelA, demonstrating the presence of RelA in Sp1 immunoprecipitates.